The leaving group in Au(I)-phosphine compounds dictates cytotoxic pathways in CEM leukemia cells and reactivity towards a Cys2His2 model Zinc Finger

Journal:	*Dalton Transactions*
Manuscript ID	DT-ART-03-2020-001136.R1
Article Type:	Paper
Date Submitted by the Author:	21-Apr-2020
Complete List of Authors:	de Paiva, Raphael; University of Sao Paulo, Fundamental Chemistry; UNICAMP, Inorganic Chemistry; VCU, Chemistry Peterson, Erica; VCU, Chemistry; VCU Massey Cancer Center Du, Zhifeng; Huazhong University of Science and Technology, Tongji School of Pharmacy; VCU, Chemistry Farrell, Nicholas; VCU, Chemistry; VCU Massey Cancer Center

ARTICLE

The leaving group in Au(I)-phosphine compounds dictates cytotoxic pathways in CEM leukemia cells and reactivity towards a Cys₂His₂ model Zinc Finger

Raphael E. F. de Paiva,[a,b]* Erica J. Peterson,[b,c] Zhifeng Du[b,d] and Nicholas P. Farrell[b,c]*

Gold(I)-phosphine "auranofin-like" compounds have been extensively explored as anticancer agents in the past decade. Although potent cytotoxic agents, the lack of selectivity towards tumorigenic vs non-tumorigenic cell lines often hinders further application. Here we explore the cytotoxic effects of a series of $(R_3P)AuL$ compounds, evaluating both the effect of the basicity and bulkiness of the carrier phosphine (R = Et or Cy), and the leaving group L (Cl⁻ *vs.* dmap). $[Au(dmap)(Et_3P)]^+$ had an IC$_{50}$ of 0.32 μM against the CEM cell line, with good selectivity in relation to HUVEC. Flow cytometry indicates reduced G1 population and slight accumulation in G2, as opposed to auranofin, which induces a high population of cells with fragmented DNA. Protein expression profile sets $[Au(dmap)(Et_3P)]^+$ further apart from auranofin, with proteolytic degradation of caspase-3 and poly(ADP-ribose)-polymerase (PARP), DNA strand-break induced phosphorylation of Chk2 Thr68 and increased p53 ser15 phosphorylation. The cytoxicity and observable biological effects correlate directly with the reactivity trend observed when using the series of gold(I)-phosphine compounds for targeting a model zinc finger, Sp1 ZnF3.

Introduction

Auranofin is one of the most successful drugs of the $\{(Et_3P)Au(I)L\}$ general structure, approved by the FDA for the treatment of rheumatoid arthritis. In a repurposing effort it has been extensively tested as an anticancer drug throughout the past decade. Regardless of the potent cytotoxicity observed for auranofin, there are many reports on lack of selectivity[1] Early mechanistic studies evidenced that auranofin and the precursor $[AuCl(Et_3P)]$ affect mitochondrial function,[2] resulting in programmed cell death rather than inducing growth arrest.[3] Auranofin induces mitochondrial swelling and loss of membrane potential, which are related to the thioredoxin/thioredoxin reductase (Trx/TrxR) system.[4,5] Auranofin is a more potent inhibitor of mitochondrial TrxR than $[AuCl(Et_3P)]^6$ but $[AuCl(Et_3P)]$ is still highly cytotoxic. Differences in the inhibition of TrxR points to different mechanisms of cytotoxicity between the two compounds. With this we exemplify the possibility of exploring the chemistry of the leaving group L as a modulator of the overall reactivity of the $(R_3P)Au(I)L$ compounds with target biomolecules, directly affecting the cytotoxicity of the compound as consequence.

Inspired by the structure of auranofin, we aimed to evaluate the cytostatic and cytotoxic mechanisms of a series of Au(I)-phosphine compounds (Figure 1). This series was designed considering that the very same aspects that govern reactivity at the molecular level, such as the basicity and bulkiness of the phosphine ligand (Et₃P vs. Cy₃P), σ-donating properties and substitution lability of the formal leaving groups L (L=Cl⁻ or 4-dimethylaminopyridine, dmap) and overall charge of the
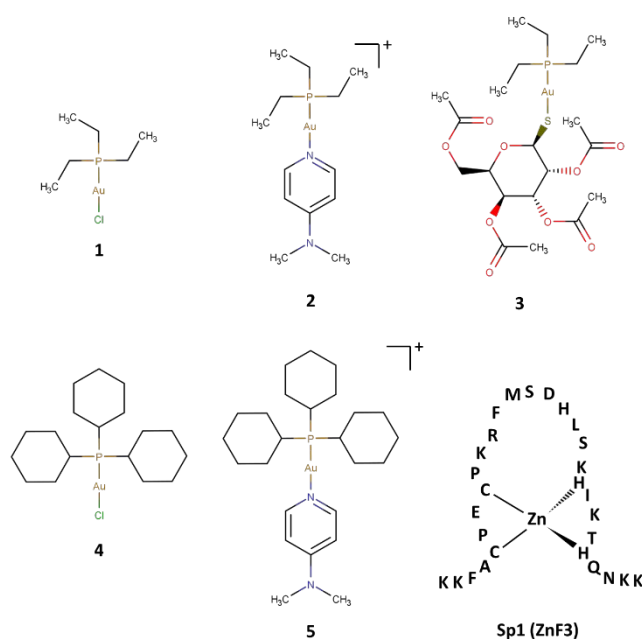
a. *Department of Fundamental Chemistry, Institute of Chemistry, University of Sao Paulo (USP), Sao Paulo, SP 05508-000, Brazil.*

b. *Department of Chemistry, Virginia Commonwealth University, Richmond, VA 23284-2006, USA.*

c. *The Massey Cancer Center, Virginia Commonwealth University, Richmond 23294, Virginia, USA*

d. *Tongji School of Pharmacy, Huazhong University of Science and Technology, Wuhan, Hubei 430030, China*

*raphael.enoque@gmail.com, *npfarrell@vcu.edu

Figure 1. List of cytotoxic gold(I)-phosphine compounds evaluated in this study (**1**, **2**, **4** and **5**), in comparison to auranofin (**3**). The structure of the third Zinc Finger of the transcription factor Sp1 is also shown.

compounds are also expected to play a role in the overall cytotoxic response of the compounds.

This study focuses on evaluating the cytotoxic effects of the Au(I)-phosphine compounds on the T lymphocytic leukemia cell line (CEM). This cell line was chosen by inspiration from a recently concluded Phase I and Phase II clinical trial that evaluated auranofin (**3**) for the treatment of Chronic Lymphocytic Leukemia (see clinicaltrials.gov, identifier NCT01419691). The classical work by Mirabelli and co-workers also demonstrated that, of a selection of 15 mouse tumour models, auranofin was active only against P388 leukemia.[7] We picked the non-tumorigenic cell line HUVEC (human umbilical vein endothelial cells) was studied for comparison, to determine selectivity. To further understand the factors governing cytotoxicity, cell uptake of Au, cell cycle analysis and determination of apoptosis-related protein expression profile were evaluated.

Furthermore, the intrinsic thiophilicity of gold(I) enables a chemoselectivity towards Cys-containing proteins. The correlation between chemical structure and reactivity of the compounds with model biomolecules such as N-Ac-Cys and the viral HIV-1 NCp7 ZnF was discussed in details in our recent works.[8,9] Expanding on this context, we studied the interaction of our series of Au(I)-phosphine compounds with the third zinc finger of the transcription factor Sp1 (Sp1 ZnF3). Under a basic science perspective, Sp1 ZnF3 is a short (28 amino acids-long) peptide model, representing an excellent platform for exploring the reactivity of the gold(I) compounds. It is also noteworthy that Hanahan and Wenberg defined 8 essential cellular pathways (hallmarks) for tumorigenesis and cancer progression: sustained proliferative signaling, replicative immortality, resistance to cell death and avoidance of immune destruction, induction of angiogenesis, invasion and metastasis and de-regulation of cellular energetics.[10,11] Sp1 levels correlate with stage, invasiveness and metastatic degree. High levels are recently being associated with poor prognosis. Based on the combination of these factors, Sp1 is an interesting target for cancer therapy.[12]

Experimental

Materials

Tricyclohexylphosphine, 4-dimethylaminopyridine (dmap), 2,2'-thiodiethanol and auranofin were obtained from Sigma-Aldrich. $H[AuCl_4]$ and triethylphosphine (Et_3P) were purchased from Acros. Chemicals were used without further purification. The Sp1 ZnF3 peptide (KKFA**C**PE**C**PKRFMSDHLSK**H**IKT**H**QNKK) was purchased from GenScript Corporation (USA).

Synthesis of the Au(I)-phosphine compounds

Compounds **1**, **2**, **4** and **5** were synthesized as described recently by us.[8] Briefly, the parent chloro(phosphine)gold(I) compounds (**1** and **4**) were obtained through reduction of $H[AuCl_4]$ with 2,2'-thiodiethanol followed by addition of the respective phosphine ligand. The chloride ligand was then replaced (compounds **2** and **5**) firstly by activating the parent gold(I)-phosphine compound with silver nitrate, filtering off the white precipitate and adding

dmap. Purity was determined by CHN microanalysis and NMR spectroscopy (^{1}H and ^{31}P).[8]

Cytotoxicity assay

Human umbilical vein epithelial cells (HUVECs) were seeded in 96-well plates (5000 cells/well) containing 100 μL of Vasculife Endothelial Media (Lifeline) and allowed to attach overnight at 37 °C in 5% CO_2. The cells were treated with various concentrations of compounds **1-5** in sets containing 4 replicates per concentration. After 72 h, the media was removed and 0.5 mg mL^{-1} MTT (3-(4,5-dimethylthiazol-2-yl)-2,5-diphenyltetrazolium bromide) (Sigma) was added to each well and incubated for 3 h at 37°C. The MTT reagent was removed and 100 μL of dmso were added to each well. Spectrophotometric readings were determined at 570 nm using a Synergy H1 microplate reader (BioTek). Percent cell survival was determined as treated/untreated controls × 100. The T lymphoblast cell line, CCRF-CEM, was seeded in 96-well plates (5000 cells/well) containing 100 μL of RPMI media. The cells were treated the same as above and assayed using the Cell Counting Kit 8 (Dojindo) according to the manufacturer's instructions.

Cellular morphology

1×10^5 CEM cells were seeded in 100 mm dishes containing RPMI media and treated with IC_{25} and IC_{75} concentrations of the Au(I)-phosphine compounds. Cells were incubated at 37 °C (TC incubator) for 24 hours. Images were acquired and processed using an Olympus IX70 inverted light microscope coupled with CellSens digital imaging software.

ICP-MS analysis of Au cellular accumulation

Following the same experimental conditions described for the cytotoxicity assay, but in a larger scale, 1×10^6 CEM cells were seeded in 100 mm dishes containing RPMI media and treated with 0.18 μM of each compound for 10 min, 1.5 h or 3 h. Cells were harvested and washed twice with PBS. Cell pellets were digested overnight using 1 mL of conc. HNO_3 and diluted to 2 mL with water. Quantitation of Au content for each sample was analyzed using the Varian 820-MS ICP Mass Spectrometer. An 8-point standard curve (ranging from 100 to 0.7813 ppb) was generated for each experiment.

Cell cycle analysis using flow cytometry

1×10^6 CEM cells were seeded in 100 mm dishes containing RPMI media. Cells were treated with IC_{75} concentrations of each compound and incubated for 6 or 24 h at 37 °C. Both floating and attached cells were harvested, washed, and resuspended in 1 mL of propidium iodide solution (3.8 mmol L^{-1} sodium citrate; 0.05 mg/mL propidium iodide; 0.1% Triton X-100) with added RNase B (7 Kunitz units/mL). After staining, the solutions were passed through 35 μm filters. The samples (20,000 events each) were immediately analyzed at 670 nm by flow cytometry using a BD FACSCanto II flow cytometer and FACSDiva software.

Antibody array analysis of phospho-protein expression

The PathScan Stress and Apoptosis Signaling Antibody Array Kit (Cell Signaling) was used according to the manufacturer's instructions. Briefly, 2 x 10^6 CEM cells were seeded in two 100 mm dishes per sample and allowed to attach overnight. The cells were treated with IC_{75} concentrations of each compound for 6h. The cells were washed, harvested on ice, and lysed in the presence of protease and phosphatase inhibitors. The amount of protein for each sample was quantified using the Bradford assay. Blocking buffer was added to each array for 15 min. at room temperature, removed and replaced with 75 µg of protein overnight at 4°C. After removal of the protein, arrays were washed, and detection antibody cocktail supplied with the kit was added for 1 h at room temperature. The arrays were washed and incubated for 30 min with HRP-linked Streptavidin solution at room temperature. Finally, the slide was covered with lumiGLO/Peroxide reagent and the chemiluminescent array images were captured on film following 3–5 s exposure times. The density of the spots was quantified using the Protein Array Analyzer by ImageJ and normalized to the α-tubulin values for each sample. The difference in protein expression between the untreated control and treated samples is expressed as $\log_2$ of fold-change (normalized treated sample / normalized untreated control sample). The results discussed and expressed here are consistent with two independent runs.

Sp1 (ZnF3) preparation and targeting followed by Mass Spectrometry.

An adequate amount of apo-Sp1 (ZnF3) was dissolved in water. 1.2 equivalents of zinc acetate were added per zinc core. The pH was adjusted to 7.2-7.4 using a solution of NH_4OH. The solution was incubated for 2 h at 37 °C prior to any other experiments. The ZnF formation was confirmed by circular dichroism and mass spectrometry. The overall CD profile and species distribution in MS were in agreement with data previously reported for all ZnFs studied here.[8,13] For mass spectrometry experiments, 1 mM reaction mixtures (1:1 Au complex : Sp1 ZnF3) were prepared in water/acetonitrile mixtures at pH 7.0 (adjusted using NH_4OH). Experiments were carried out on an Orbitrap Velos from Thermo Electron Corporation operated in positive mode. Samples (25 µL) were diluted with methanol (225 µL) and directly infused at a flow rate of 0.7 µL/min using a source voltage of 2.30 kV. The source temperature was maintained at 230°C throughout the experiment.

Results and Discussion

Cytotoxicity

The growth inhibition profiles of CEMs and HUVECs treated with the five Au(I)-phosphine compounds were evaluated. The IC_{50} values (Table 1) were lower for CEMs than for HUVECs for the newly designed compound in the series (**1**, **2**, **4** and **5**), indicating the selectivity of the Au(I)-phosphine compounds towards the tumorigenic cell line over the normal one. Auranofin, on the other hand, had no selectivity between the two cell lines and was marginally more cytotoxic against the

non-tumorigenic HUVEC cell line (statistically nonsignificant). Growth inhibition curves are shown in Figure S1.

Table 1. Summary of the cytotoxic profile of the Au(I)-phosphine compounds as observed at a 72h exposure regimen.

Compound	IC_{50} / µmol L^{-1}		Relative Index
	HUVEC	CEM	
[AuCl(Et$_3$P)]	6.77 ± 0.15 [****]	1.54 ± 0.06 [*]	0.23
[Au(dmap)(Et$_3$P)]$^+$	18.44 ± 0.92	0.32 ± 0.01	57.53
Auranofin	2.13 ± 0.08 [****]	2.91 ± 0.48 [****]	0.73
[AuCl(Cy$_3$P)]	8.39 ± 0.34 [****]	1.29 ± 0.08	6.50
[Au(dmap)(Cy$_3$P)]$^+$	3.59 ± 0.39 [****]	1.35 ± 0.05	2.66

2-way ANOVA significant comparisons of [Au(dmap)(Et$_3$P)]$^+$ within each column. [*]p=0.0187; [****]p <0.0001

Compound [Au(dmap)(Et$_3$P)]$^+$ presented a >57 x relative cytotoxicity towards the tumorigenic CEM cell line. The unique profile of cytotoxicity observed for **2** is translated from a unique chemical reactivity within the Au(I)-phosphine series studied here.

Figure S2 shows the morphology of CEM cells untreated and treated with compounds **1**-**3**. Untreated CEMs have a distinguished feature of forming clusters of cells, that are disrupted upon treatment with the Au(I)-phosphine compounds. A larger amount of cellular debris and non-intact cells can be observed for treatment with compound [AuCl(Et$_3$P)]. Treatment with compound **2** led to the larger number of intact cells, while treatment with auranofin induced aggregation in the cytoplasm but most cells remained with intact cellular membranes.

Due to the potent cytotoxic effect observed for the Au(I)-phosphine series (µM to sub-µM range) against the CEMs, the analysis of cell cycle progression and apoptosis, Au intracellular accumulation and protein expression profile were studied to understand the induced mechanism of growth inhibition and cell death.
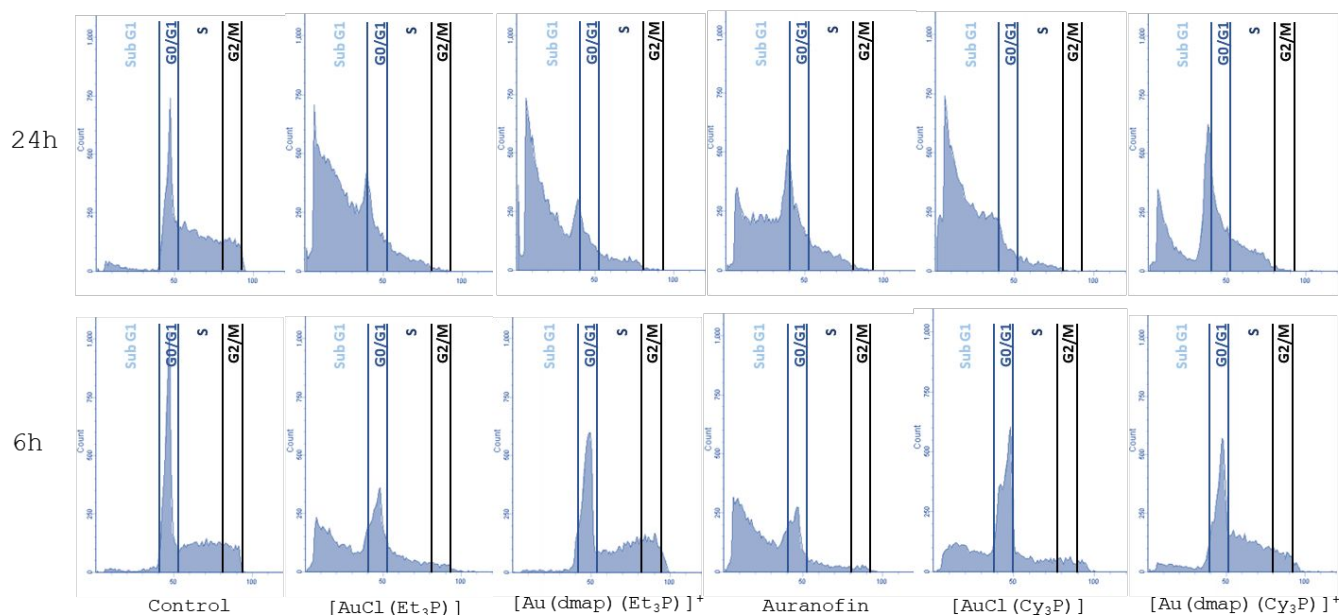
Cell Cycle Analysis

Figure 3. Flow cytometry profile of CEM cells treated with IC_{75} concentrations for 24 hours, highlighting the highly apoptotic response caused by the Au(I)-phosphine series and for 6 hours, showing differences within the series.

Flow cytometry was used to asses cell cycle changes in CEMs treated with Au(I)-phosphine compounds. In CEMs exposed to Au(I)-phosphine compounds at IC_{75} concentrations for 24h, accumulation of cells containing fragmented DNA in the sub-G1 region was observed, suggesting the induction of apoptosis (Figure 2). The apoptosis-inducing behaviour is clearly observed at the sub-G1 region. Cells treated with compound [Au(dmap)(Cy$_3$P)]$^+$ (**5**) were the least affected, but still with a high population in the sub-G1 region when compared to control. CEMs exposed to IC_{75} concentrations for 6h gave much more information regarding the mechanism of action of the tested compounds (Figure 2B). Auranofin and compound **1** had a similar apoptotic effect, with a high population of cells with fragmented DNA. Both Cy$_3$P containing compounds (**4** and **5**) induced slight changes in the G1/S transition when compared to control. Cells treated with compound [Au(dmap)(Et$_3$P)]$^+$ (**2**) presented a particularly distinguished behaviour, with reduced G1 population and a slight accumulation in G2. This behaviour is indicative of a different mechanism of cell death, since the G2 arrest is often a result of DNA damage or mitotic catastrophe. Flow cytometry data obtained for treatments with IC_{25} for 6 hours can be found in Figure S3

As a comparison, previous studies indicated that B16 melanoma cells treated with auranofin in the range 0.0125-0.2 μM for 24 hours led to 90% or greater cell survival, with no changes from the control experiment observed in the DNA distribution histograms. Treatments with 0.2 μM and higher concentrations led to extensive cellular lysis. Auranofin showed no selectivity against cycling versus noncycling cells.[14]

Cellular uptake of Au

Drug effectiveness is often related to intracellular uptake, making it an important parameter for drug design and development. The cellular uptake of metallodrugs can be
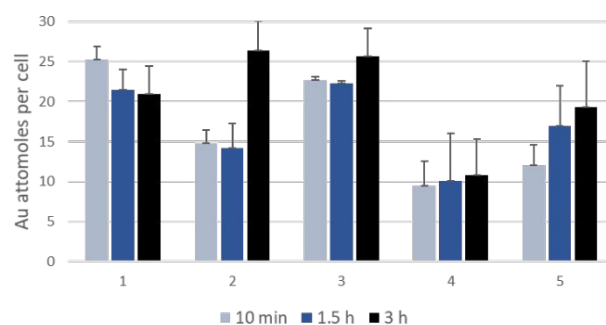

Figure 2. Au accumulation in CEM cells treated with compounds [AuCl(Et$_3$P)] (**1**), [Au(dmap)(Et$_3$P)]$^+$ (**2**), Auranofin (**3**), [AuCl(Cy$_3$P)] (**4**) and [Au(dmap)(Cy$_3$P)]$^+$ (**5**).

directly quantified by means of instrumental techniques such as inductively coupled plasma mass spectrometry (ICP-MS). Intracellular quantities of Au in CEMs treated with equimolar sub-IC_{50} (0.18 μM) amounts of each compound for 10 min, 1.5h, and 3h, show structural trends correlating with the size of the phosphine ligands (Figure 2). Et$_3$P-containing compounds (**1**, **2** and **3**) have a higher final accumulation than Cy$_3$P-containing compounds (**4** and **5**). A clear increase in Au uptake was observed for the cationic compounds (**2** and **5**) from 10 min to 3h, but not for the neutral compounds [AuCl(Et$_3$P)], auranofin and [AuCl(Cy$_3$P)]. A comparison between the IC_{50} values from Table 1 and intracellular gold levels determined by ICP-MS in CEM cells (Figure 2) reveals that there is no direct correlation between the two. The total amount of intracellular gold is not the only factor that can govern cytotoxicity. To further assess the effect of the gold(I)-phosphine series on CEM cells, protein expression levels were evaluated.

As a comparison, the interaction of [AuCl(Et$_3$P)] and auranofin with RAW 264.7 macrophages has been described in the literature.[15] The interaction of the compounds with the

ARTICLE

target cell line was evaluated on [195]Au-labeled compounds. A higher Au uptake was observed in RAW 264.7 cells treated with [AuCl(Et$_3$P)] than with auranofin. The time course of the cellular association of the [195]Au-labeled compounds with RAW 246.7 cells was also studied. The [195]Au content was evaluated up to 60 min incubation. The total [195]Au content increased for up to 20 min and then started to drop, as did the total number of cells (cytotoxic effect). The incorporation of Au from [AuCl(Et$_3$P)] was higher than from auranofin.[15]
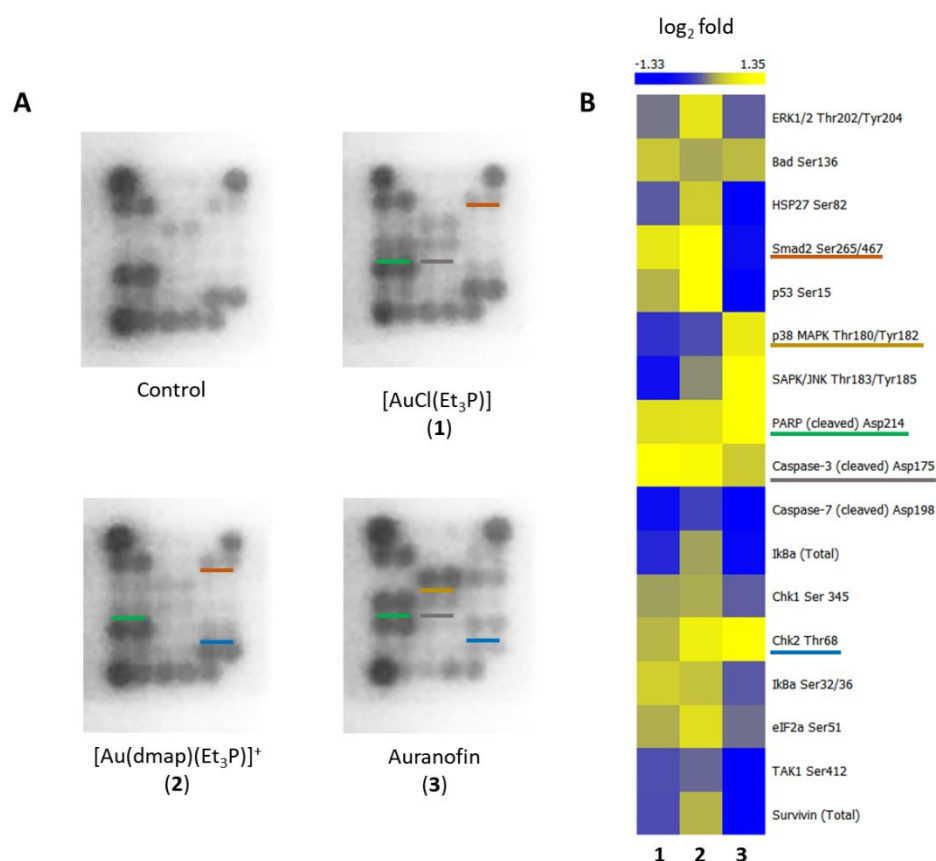
Protein Expression Profile

Regarding molecular targets, [AuCl(Et$_3$P)] was shown to bind to DNA,[16] as opposed to auranofin. A series of Au(I)-triethylphosphine complexes, including auranofin, was shown to inhibit cytosolic and mitochondrial thioredoxin reductase,[17] the most recurring target in the literature for this class of compounds. Some other explored targets include glutathione-S-transferase, which was inhibited by auranofin;[18] lymphoid tyrosine phosphatase (over other tyrosine phosphatases), reported to be inhibited by chlorido(cyanoethyl)phosphinegold(I);[19] the proteasome, with all three enzyme activities (chymothryptic-like, caspase-like and tryptic-like) inhibited in the micromolar range by [(pbiH)Au(PPh$_3$)]PF$_6$ (pbiH = 2-(pyridin-2-yl)-1H-1,3-benzimidazole),[20] and not by auranofin. As demonstrated here, a wide range of possible molecular targets are available for Au(I)-phosphine compounds, with important consequences for cytotoxic selectivity.

The relative expression of 19 cell stress and apoptosis-related phosphoproteins in response to 6h IC$_{75}$ treatments of CEMs with auranofin, [AuCl(Et$_3$P)] and [Au(dmap)(Et$_3$P)]$^+$ was compared using a phospho-antibody array (Figure 4A). Quantification using densitometric analysis is also shown

(Figure 4B). The Pathscan Stress and Apoptosis Signalling antibody array kit with chemiluminescent readouts simultaneously detect the cleavage of poly (ADP-ribose) polymerase (PARP) (Asp214), caspase-3 (Asp175) and caspase-7 (Asp198); phosphorylation of extracellular signal-regulated kinase (ERK)-1/2 (Thr202/Tyr204), protein kinase B (Akt; Ser473), BCL-2-associated death promoter (Bad; Ser136), heat shock protein 27 (HSP27; Ser82), Smad2 (Ser465/467), p53 (Ser15), p38 mitogen activated protein kinase (p38 MAPK; Thr180/Tyr182), stress-activated protein kinases and Jun amino-terminal kinases (SAPK/JNK; Thr183/Tyr185), checkpoint kinase 1 (Chk1; Ser345), checkpoint kinase 2 (Chk2; Thr68), NF-κB inhibitor α (IκBα Ser32/36), eukaryotic translation initiation factor 2 subunit α (eIF2; Ser51) and transforming growth factor-β-activated kinase 1 (TAK1) (Ser412) and determination of protein content of IκBα, survivin and α-tubulin. These signalling molecules represent a good starting point for probing the mechanism of cell death when studying a new cytotoxic agent.

The series containing triethylphosphine was selected because it demonstrated better selectivity towards the tumorigenic cell line and compound **2** exhibited the highest cytotoxicity among the compounds discussed here. For all three compounds, proteolytic degradation of caspase-3 was observed, an important substrate of intrinsic (caspase-9) and extrinsic (caspase-8) mediators of apoptosis. This was accompanied by proteolytic degradation of poly(ADP-ribose)-polymerase (PARP), a downstream indicator of cells in the final stage of apoptotic DNA fragmentation. DNA strand-break induced phosphorylation of Chk2 Thr68 was apparent for all three compounds, however only [Au(dmap)(Et$_3$P)]$^+$ showed a concomitant increase in p53 ser15 phosphorylation and G2-arrest at this time point. It is possible that auranofin and [AuCl(Et$_3$P)] also induce p53 phosphorylation and cell cycle arrest, but at earlier time points. Indeed, for these two

Figure 4. A. CEM cells either untreated (control) or treated with IC$_{75}$ concentrations of Au(I)-phosphine compounds **1-3** for 6h. Cell lysates were analyzed with the PathScan stress and apoptosis signaling antibody array kit. B. Densitometric protein profile of CEM cells treated with compounds **1-3,** expressed as log$_2$ of fold change.

compounds, the percentage of cells in the sub-G1 fraction is higher than for [Au(dmap)(Et₃P)]⁺ suggesting a faster rate of cell death (see Figure 2B). As observed in Figure 2, although the final concentration of gold per cell is similar for the 3 compounds evaluated, [AuCl(Et₃P)] and auranofin had a higher accumulation at earlier time points, while [Au(dmap)(Et₃P)]⁺ took a longer time to reach the final concentration observed. These observations are suggestive of an alternative mechanism of cell death for [Au(dmap)(Et₃P)]⁺, a direct consequence of the slower chemical reactivity achieved by replacing the labile chloride by dmap.

CEM cells treated with auranofin showed increased phosphorylation of p38 MAPK (Thr180/Tyr182) and SAPK/JNK (Thr183/Tyr185), as previously reported for HL-60 leukemia cells.[21] This result is consistent with the well-documented cellular response to the increase of reactive oxygen species due to inhibition of cytosolic and mitochondrial thioredoxin reductase (TrxR).[22,23] On the other hand, [Au(dmap)(Et₃P)]⁺ showed elevated levels of Smad2/3 (Ser465/467) phosphorylation when compared to the untreated control, while Auranofin showed the opposite result. Although we cannot be certain Smad2/3 is not activated at earlier or later time points in this system, to our knowledge increases in Smad2/3 phosphorylation have never been reported for auranofin. Smad2 and Smad3 become phosphorylated at their carboxyl termini by the receptor kinase TGF-β Receptor I following stimulation by TGF-β. Recent reports correlate activation of TGF-β with induction of apoptosis.[24,25] Latent TGF-β acts as an extracellular sensor of oxidative stress. Release of active TGF-β from the latent complex binding protein (LTBP) and latency associated peptide (LAP) occurs in response to a variety of agents such as heat, acidic pH, chaotropic agents, and reactive oxygen species.

ERK1 and ERK2 are protein-serine/threonine kinases that participate in the Ras-Raf-MEK-ERK cascade. This cascade is responsible for regulating a large variety of cellular processes, mainly proliferation and survival but also including adhesion, cell cycle progression, migration and differentiation.[26] The ERK1/2 catalyzed phosphorylation of nuclear transcription factors requires the translocation of ERK1/2 into the nucleus by active and passive processes involving the nuclear pore. These transcription factors participate in the immediate early gene response. Auranofin and [AuCl(Et₃P)] led to ERK1/2 phosphorylation levels similar to that of the untreated control. On the other hand, increased ERK1/2 phosphorylation was observed for CEM cells treated with [Au(dmap)(Et₃P)]⁺. Although ERK1/2 phosphorylation generally promotes cell survival, it has been shown that under certain circumstances of DNA damage stimuli, ERK1/2 can have pro-apoptotic functions. For example, ERK promotes p53 stability by phosphorylation on Ser15,[27,28] leading to its accumulation by inhibition of the association with Mdm2.[29] CEM cells treated with [Au(dmap)(Et₃P)]⁺ had both ERK 1/2 and p53 phosphorylation upregulated. Furthermore, it has been hypothesized that the main cause of ERK sustained activation is the presence of ROS.[30] Finally, HSP27 is a mediator of cell stress, conferring resistance to adverse conditions, being activated by phosphorylation at

Ser82. CEM cells treated with [Au(dmap)(Et₃P)]⁺ had a significant increase in HSP27 phosphorylation, which is not observed for treatment with [AuCl(Et₃P)]. A significant HSP27 phosphorylation induction was also recently observed when HT-29 cells were treated with organometallic Au(I)(triphenylphosphine) compounds containing alkynyl and N-heterocyclic carbene ligands.[31,32] HSP27 activation, along with eIF2, is consistent with a mechanism based on extracellular oxidative stress.

Chemical Reactivity towards the Cys₂His₂ Model Zinc Finger Sp1 ZnF3

We have previously demonstrated the importance of ZnF-targeting on the biological effects of gold(I)-phosphine compounds.[8,9,33] Here we expand the scope of this chemistry to the human transcription factor Sp1, one of the "hallmarks" of cancer.[11,12]

The interaction of the Au(I)-phosphine series with Sp1 (ZnF3) was followed by mass spectrometry. The reaction proceeds quickly and we discuss the products observed immediately upon incubation. [AuCl(Et₃P)]⁺ (**1**) reacts immediately with Sp1 (F3) as observed by a clean mass spectrum (Figure 5A), yielding only AuF in multiple charge states as a product (AuF⁶⁺, 594.96 m/z; AuF⁵⁺, 713.75 m/z; AuF⁴⁺, 891.93 m/z and AuF³⁺, 1188.91 m/z). This is indicative of a mechanistically well-defined reaction between the Au(I)-phosphine compound, causing Zn(II) displacement along with Au(I) incorporation. [Au(dmap)(Et₃P)] (**2**) reacts faster with Sp1 ZnF3, as opposed to what is observed when targeting the viral HIV-1 NCp7 ZnF2.[8] Here many AuF-related species can be observed, in analogy to what is observed for compound **1** (AuF⁶⁺, 594.96 m/z; AuF⁵⁺,713.75 m/z; AuF⁴⁺, 891.93 m/z and AuF³⁺, 1188.91 m/z). However, it can be considered the least reactive compound within the series of compounds studied here, as a heterobimetallic species Au-ZnF can still be observed (Figure 5B). To some extent, peptide oxidation is also observed, given the presence of the oxidized species oxiF⁵⁺ (674.15) and oxiF⁴⁺ (842.44).
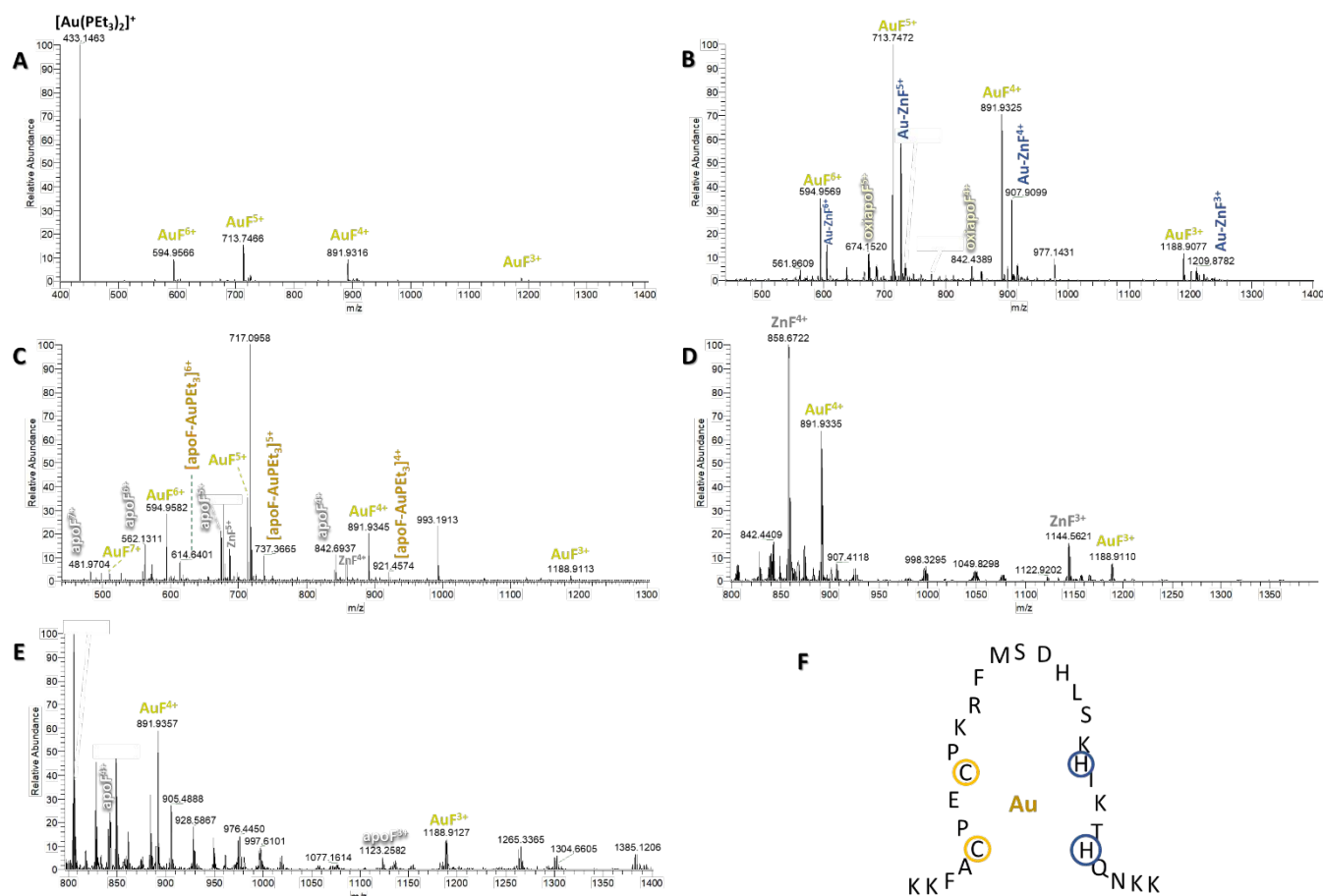
Figure 5. ESI-MS spectrum (positive mode) for the reaction between Sp1 (ZnF3) and [AuCl(Et₃P)]⁺ (**A**), [Au(dmap)(Et₃P)]⁺ (**B**), auranofin (**C**), [AuCl(Cy₃P)]⁺ (**D**) and [Au(dmap)(Cy₃P)]⁺ (**E**) immediately upon incubation at a 1:1 molar ratio between the gold complexes and the target ZnF. The AuF species formed upon interaction of [AuCl(Et₃P)]⁺ and [Au(dmap)(Et₃P]⁺ with Sp1 ZnF3 were subjected to MS/MS analysis and the coordination sphere in both cases is Cys(S)-Au-N(His), as represented in **F**. Either one of the Cys residues highlighted in yellow, and either of the His residues marked in blue are expected to bind Au(I), as evidenced by MS/MS (See Figures S4 and S5).

Auranofin (**3**) interacts with Sp1 ZnF3 producing a much wider variety of Au-containing species immediately after incubation (Figure 5C). AuF species were identified, such as AuF⁶⁺, AuF⁵⁺, AuF⁴⁺ and AuF³⁺. Non-metallated peptide was identified, in the form of apoF⁶⁺, apoF⁵⁺ and apoF⁴⁺. Interestingly auranofin presented some reaction products where the phosphine ligand remained coordinated to Au(I), as exemplified by species such as Et₃PAuF⁶⁺ (614.64), Et₃PAuF⁵⁺ (737.37) and Et₃PAuF⁴⁺ (921.46), in the same way as previously reported by us for a Au(I)-triphenylphosphine series.[33]

When replacing Et₃P by the more basic and sterically hindered Cy₃P, more differences can be observed. [AuCl(Cy₃P)]⁺ was less reactive than [AuCl(Et₃P)]⁺ when targeting Sp1 ZnF3, as unreacted ZnF can still be observed. Some gold incorporation can also be observed, as diagnosed by the presence of AuF peaks such as AuF⁴⁺ and AuF³⁺ (Figure 5D). The replacement of Cl⁻ by dmap further tunes the reactivity. For the reaction of [Au(dmap)(Cy₃P)] (**5**) with Sp1 ZnF3, three remarks can be made: no unreacted ZnF is observed; apo-peptide is present (apoF⁴⁺ and apoF³⁺), and gold is also incorporated (AuF⁴⁺ at 891.94 and AuF³⁺ at 1188.91 m/z).

The AuF species formed by the interaction of [AuCl(Et₃P)] and [Au(dmap)(Et₃P)] with Sp1 ZnF3 were also subjected to

Collision-Induced Dissociation. For AuF species observed upon interaction of [Au(dmap)(Et₃P)]⁺ with Sp1 ZnF3, the parent ion at 891.6 m/z (AuF⁴⁺) was fragmented with 30 eV (Figure S4). Two internal fragments and one N-terminal fragment are observed to bind with gold, which indicates the auration of cysteine and histidine in AuF species. For being a relatively large peptide, the energy required to induce fragmentation of Sp1 ZnF3 is not low enough to allow the observation of Au(I) adducts with shorter peptide fragments. Although a definitive binding assignment cannot be made, the final coordination sphere of the incorporated Au(I) is Cys(S)-Au-N(His), as shown in Figure 5F. The AuF³⁺ parent ion at 1188.90 m/z formed by the reaction of [AuCl(Et₃P)] with Sp1 ZnF3 was subjected to CID under the same conditions (Figure S5). Similarly, aurated internal fragments and N-terminal fragment indicate a Cys(S)-Au-N(His) coordination sphere. The binding site assignment obtained here by CID are in agreement with Travelling Wave Ion Mobility-Mass Spectrometry studies on the AuF obtained upon the interaction of [AuCl(Et₃P)] and Sp1 ZnF3.[34]

A clear parallel can be drawn between the reactivity trends observed for the Au(I)-phosphine series towards the model Sp1 ZnF3 and the cytotoxic profile. For [Au(dmap)(Et₃P)]³⁺ (**2**) the fine-tuned reactivity obtained by the combination of the Et₃P

carrier with the dmap leaving group produced a unique response upon interaction with Sp1 ZnF3. For example, it was the only compound in the series that has a heterobimetallic adduct with the peptide (Figure 5B), indicating a lower reactivity when targeting Sp1 ZnF3. Biologically, both auranofin and [AuCl(Et₃P)] induce a high population of CEM cells to the sub-G1 fraction, as opposed to [Au(dmap)(Et₃P)]⁺, suggesting a slower rate of cell death for the latter. The concentration of gold per cell is similar for the three Et₃P-Au(I) compounds, but [AuCl(Et₃P)] and auranofin had a higher accumulation at earlier time points, while [Au(dmap)(Et₃P)]⁺ took a longer time to reach the final concentration observed.

Our studies here indicate that the Cys₂His₂ Sp1 ZnF3 is intrinsically more reactive than another zinc finger recently studied by us, the viral Cys₂HisCys HIV-1 NCp7 ZnF2.[8] As the prototypical gold(I)-based drug, auranofin has been studied extensively in the literature as a ZnF inhibitor, which allows us to draw interesting comparisons. In a recent study, we identified through MS/MS data that auranofin interacts with HIV-1 C-terminal ZnF domain (ZnF2), producing aurated fragments that are diagnostic for Au-His binding, as well as fragments associated with the expected Au-Cys binding. The observation of only (PEt₃)Au-His binding in the full NC, whereas both [(PEt₃)Au-Cys] and [(PEt₃)Au-His] species appear for the C-terminal finger is an important evidence that indicates that the environment of the cysteines directs Au(I) binding. In another study, it was demonstrated that auranofin reacted slowly with a Cys₂His₂ apopeptide without Zn displacement observed from the Zn-peptide.[35] Finally, monoadduct {AuF} species were identified by mass spectrometry when auranofin reacts with a Zn(Cys₂HisCys) model from a PARP sequence but not with the apopeptide.[36] We also recently studied the interaction of Sp1 ZnF3 with cisplatin and the analog [PtCl₂(en)] (en=ethylenediamine).[13] Another interesting comparison can be drawn between the R₃PAuL series studied here with the (dien)Au(III)L compounds,[37] were the tridentate dien ligand also works as a carrier ligand for Au(III), in analogy to the phosphines used for Au(I) here. Noncovalent adducts, enabled by π-π interactions between [Au(dien)(dmap)]³⁺ and aromatic residues, were found when targeting the full HIV-1 NCp7 nucleocapsid,[9] which further demonstrates the reactivity tuning caused by dmap. [PtCl₂(en)] was found to react faster than cisplatin wth Sp1 (ZnF3), as observed by {¹H,¹⁵N}-HSQC and MS. Cisplatin was reported to be unreactive towards Sp1 ZnF2, although both zinc fingers have the same Cys₂His₂ motif. [38] Another platinum-based antitumoral agent, *trans*-[PtCl₂(NH₃)(thiazole)], was highly reactive towards Sp1 ZnF2.[39] The platination of Sp1 disrupts the secondary structure of the protein, thus interfering with its DNA recognition function. An *in cellulo* assay indicated that upon binding to Sp1, the *trans* platinum compound inhibits Sp1 trafficking from the cytoplasm to the nucleus. This combination of effects ultimately interferes with protein expression levels.[39]

Conclusions

A series of Au(I)-phosphine compounds based on the Et₃P and on the bulkier Cy₃P ligands was evaluated in terms of cytotoxicity. Two cell lines were selected, a T lymphocyte tumorigenic cell line (CEM) and the non-tumorigenic the Human Umbilical Vein Endothelial cells (HUVEC). IC₅₀ values obtained using the MTT protocol were found in lower μM range, or even sub-μM for the compound [Au(dmap)(Et₃P)]⁺. All compounds evaluated here, besides auranofin, demonstrated selectivity towards the CEM cell line. The highest selectivity (>57x) was found for [Au(dmap)(Et₃P)]⁺. High apoptotic activity was observed on CEM cells treated with each compound tested here based on flow cytometry data. CEMs exposed to IC₇₅ concentrations of compound [Au(dmap)(Et₃P)]⁺ (2) for 6h presented a particularly distinguished behaviour, with reduced G1 population and a slight accumulation in G2. This behaviour is indicative of a different mechanism of cell death, since the G2 arrest is often a result of DNA damage or mitotic catastrophe. The CEM cells treated with Et₃P-containing compounds were further evaluated by protein expression profile. The compound [Au(dmap)(Et₃P)]⁺ was shown to cause a wide range of cellular responses that trigger apoptosis (based for example on activation of Chk2, HSP27, sustained activation of ERK 1/2), as opposed to auranofin that mainly activates p38 MAPK. The sub-μM cytotoxicity observed over CEM cells is a direct consequence of this multi-modal response. The mechanism of apoptosis induced in CEM cells by treatment with [Au(dmap)(Et₃P)]⁺ is summarized in Scheme 1. For comparison, the overall mechanism of cytotoxicity caused by auranofin is given in Figure S4, which is in agreement with the apoptotic mechanism previously reported for HL-60 leukemia cells treated with auranofin.[21]
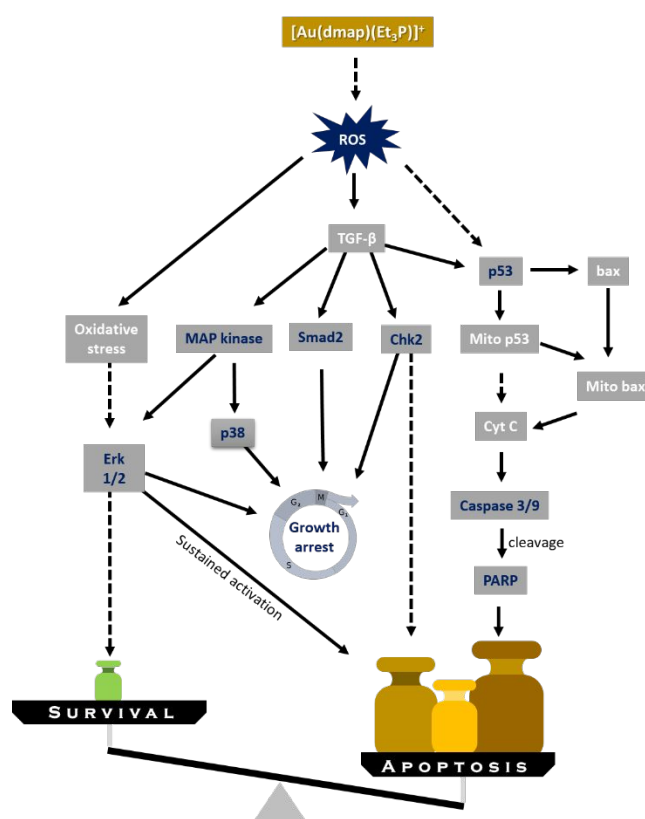
Scheme 1. Summary of the cytotoxic mechanism observed for [Au(dmap)(Et$_3$P)]$^+$ against CEM cells as observed by flow cytometry and protein expression profiles. Solid arrows represent a single step, while dashed arrows represent multiple steps. ROS formation is expected, based on previous mechanism of cell death caused by auranofin[21] and other gold(I)-phosphine compounds.[40]

The reaction of the gold(I)-phosphine series studied here towards the model Cys$_2$His$_2$ Zinc Finger Sp1 ZnF3 provided valuable chemical basis for explaining the biological effects observed in this study. [Au(dmap)(Et$_3$P)]$^{3+}$ (**2**) has a unique combination of properties coming from Et$_3$P (basicity and lower bulkiness when compared to Cy$_3$P), in combination with the less labile dmap leaving group. This combination of properties is translated to a lower reactivity towards the target biomolecule, which, as observed by the heterobimetallic adduct. Biologically, both auranofin and [AuCl(Et$_3$P)] induced a sub-G1 population on CEM cells, as opposed to [Au(dmap)(Et$_3$P)]$^+$, suggesting a slower rate of cell death for the latter. The same trend can be observed when looking at the gold uptake for the three Et$_3$P-Au(I) compounds. Both [AuCl(Et$_3$P)] and auranofin have a higher accumulation at earlier time points, while [Au(dmap)(Et$_3$P)]$^+$ took a longer time to reach the final concentration observed.

Conflicts of interest

There are no conflicts to declare.

Acknowledgements

Notes and references

1   F. Magherini, A. Modesti, L. Bini, M. Puglia, I. Landini, S. Nobili, E. Mini, M. A. Cinellu, C. Gabbiani and L. Messori, *J. Biol. Inorg. Chem.*, 2010, **15**, 573–582.

2   P. J. Barnard and S. J. Berners-Price, *Coord. Chem. Rev.*, 2007, **251**, 1889–1902.

3   M. J. McKeage, *Br. J. Pharmacol.*, 2002, **136**, 1081–1082.

4   M. P. Rigobello, G. Scutari, A. Folda and A. Bindoli, *Biochem. Pharmacol.*, 2004, **67**, 689–696.

5   M. P. Rigobello, G. Scutari, R. Boscolo and A. Bindoli, *Br. J. Pharmacol.*, 2002, **136**, 1162–1168.

6   M. P. Rigobello, M. T. Callegaro, E. Barzon, M. Benetti and A. Bindoli, *Purification of Mitochondrial Thioredoxin Reductase and Its Involvement in the Redox Regulation of Membrane Permeability*, 1998, vol. 24.

7   C. K. Mirabelli, R. K. Johnson, C. M. Sung, L. Faucette, K. Muirhead and S. T. Crooke, *Cancer Res.*, 1985, **45**, 32–9.

8   R. E. F. de Paiva, Z. Du, E. J. Peterson, P. P. Corbi and N. P. Farrell, *Inorg. Chem.*, 2017, **56**, 12308–12318.

9   C. Abbehausen, R. E. F. de Paiva, R. Bjornsson, S. Q. Gomes, Z. Du, P. P. Corbi, F. A. Lima and N. Farrell, *Inorg. Chem.*,

10   2018, **57**, 218–230.

       D. Hanahan and R. A. A. Weinberg, *Cell*, 2011, **144**, 646–74.

11   D. Hanahan and R. A. Weinberg, *Cell*, 2000, **100**, 57–70.

12   K. Beishline and J. Azizkhan-Clifford, *FEBS J.*, 2015, **282**, 224–258.

13   Z. Du, R. E. F. de Paiva, Y. Qu and N. Farrell, *Dalton Trans.*, 2016, **45**, 8712–8716.

14   C. K. Mirabelli, R. K. Johnson, C. Sung, L. Faucette, K. Muirhead and S. T. Crooke, *CANCER Res.*, 1985, **45**, 32–39.

15   R. M. Snyder, C. K. Mirabelli and S. T. Crooke, *Biochem. Pharmacol.*, 1987, **36**, 647–654.

16   C. K. Mirabelli, C.-M. Sung, J. P. Zimmerman, D. T. Hill, S. Mong and S. T. Crooke, *Biochem. Pharmacol.*, 1986, **35**, 1427–1433.

17   V. Gandin, A. P. Fernandes, M. P. Rigobello, B. Dani, F. Sorrentino, F. Tisato, M. Björnstedt, A. Bindoli, A. Sturaro, R. Rella and C. Marzano, *Biochem. Pharmacol.*, 2010, **79**, 90–101.

18   A. De Luca, C. G. Hartinger, P. J. Dyson, M. Lo Bello and A. Casini, *J. Inorg. Biochem.*, 2013, **119**, 38–42.

19   M. R. Karver, D. Krishnamurthy, N. Bottini and A. M. Barrios, *J. Inorg. Biochem.*, 2010, **104**, 268–273.

20   N. Micale, T. Schirmeister, R. Ettari, M. A. Cinellu, L. Maiore, M. Serratrice, C. Gabbiani, L. Massai and L. Messori, *J. Inorg. Biochem.*, 2014, **141**, 79–82.

21   S.-J. Park and I.-S. Kim, *Br. J. Pharmacol.*, 2005, **146**, 506–13.

22   Y. Omata, M. Folan, M. Shaw, R. L. Messer, P. E. Lockwood, D. Hobbs, S. Bouillaguet, H. Sano, J. B. Lewis and J. C. Wataha, *Toxicol. Vitr.*, 2006, **20**, 882–890.

23   Y. Omata, J. B. Lewis, P. E. Lockwood, W. Y. Tseng, R. L. Messer, S. Bouillaguet and J. C. Wataha, *Toxicol. In Vitro*, 2006, **20**, 625–33.

24   V. T. Solovyan and J. Keski-Oja, *Cell Death Differ.*, 2005, **12**, 815–826.

25   K. Richter, A. Konzack, T. Pihlajaniemi, R. Heljasvaara and T. Kietzmann, *Redox Biol.*, 2015, **6**, 344–352.

26   R. Roskoski, *Pharmacol. Res.*, 2012, **66**, 105–143.

27   W. Woessmann, X. Chen and A. Borkhardt, *Cancer Chemother. Pharmacol.*, 2002, **50**, 397–404.

28   J. Liu, W. Mao, B. Ding and C. -s. Liang, *AJP Hear. Circ. Physiol.*, 2008, **295**, H1956–H1965.

29   Q. B. She, N. Chen and Z. Dong, *J. Biol. Chem.*, 2000, **275**, 20444–9.

30   S. Cagnol and J.-C. Chambard, *FEBS J.*, 2010, **277**, 2–21.

31   V. Andermark, K. Göke, M. Kokoschka, M. A. Abu el Maaty, C. T. Lum, T. Zou, R. W.-Y. Sun, E. Aguiló, L. Oehninger, L. Rodríguez, H. Bunjes, S. Wölfl, C.-M. Che and I. Ott, *J. Inorg. Biochem.*, 2016, **160**, 140–148.

32   P. Holenya, S. Can, R. Rubbiani, H. Alborzinia, A. Jünger, X. Cheng, I. Ott and S. Wölfl, *Metallomics*, 2014, **6**, 1591–1601.

33   C. Abbehausen, E. J. Peterson, R. E. F. De Paiva, P. P. Corbi, A. L. B. Formiga, Y. Qu and N. P. Farrell, *Inorg. Chem.*, 2013, **52**, 11280–11287.

34   Z. Du, R. E. F. de Paiva, K. Nelson and N. P. Farrell, *Angew. Chemie Int. Ed.*, 2017, **56**, 4464–4467.

35   Ü. A. Laskay, C. Garino, Y. O. Tsybin, L. Salassa, A. Casini, U. A. Laskay, C. Garino, Y. O. Tsybin, L. Salassa and A. Casini, *Chem. Commun.*, 2015, **51**, 1612–1615.

36   M. A. Castiglione Morelli, A. Ostuni, G. Matassi, C. Minichino, A. Flagiello, P. Pucci and A. Bavoso, *Inorganica Chim. Acta*, 2016, **453**, 330–338.

37   S. R. Spell and N. P. Farrell, *Inorg. Chem.*, 2015, **54**, 79–86.

38   S. Chen, H. Jiang, K. Wei, Y. Liu, M. Losacco, G. Natile, Y. Z. Liu, M. Schurmann, E. C. Fusch and B. Lippert, *Chem. Commun.*, 2013, **49**, 1226.

39   S. Chen, D. Xu, H. Jiang, Z. Xi, P. Zhu and Y. Liu, *Angew. Chemie - Int. Ed.*, 2012, **51**, 12258–12262.

40   J. H. Kim, E. Reeder, S. Parkin and S. G. Awuah, *Sci. Rep.*, 2019, **9**, 1–18.

The leaving group L in $[(R_3P)AuL]^{n+}$ regulates the cytotoxic mechanism against CEM leukemia cells and the reactivity towards Sp1 ZnF3